APPLIED AND ENVIRONMENTAL MICROBIOLOGY, Feb. 2009, p. 676–686 Vol. 75, No. 3
0099-2240/09/$08.00+0 doi:10.1128/AEM.01683-08

Discovery of Stable and Variable Differences in the *Mycobacterium avium* subsp. *paratuberculosis* Type I, II, and III Genomes by Pan-Genome Microarray Analysis▽†

Elena Castellanos,[1] Alicia Aranaz,[1] Katherine A. Gould,[2] Richard Linedale,[2] Karen Stevenson,[3] Julio Alvarez,[1] Lucas Dominguez,[1] Lucia de Juan,[1] Jason Hinds,[2] and Tim J. Bull[2]*

Centro de Vigilancia Sanitaria Veterinaria, Departamento Sanidad Animal, Facultad de Veterinaria, Universidad Complutense, Madrid, Spain[1]; Division of Cellular and Molecular Medicine, St. George's University of London, Cranmer Terrace, London SW17 0RE, United Kingdom[2]; and Moredun Research Institute, Division of Control of Bacterial Diseases, Pentlands Science Park, Bush Loan EH26 0PZ, Penicuik, United Kingdom[3]

Received 21 July 2008/Accepted 21 November 2008

Mycobacterium avium* subsp. *paratuberculosis* is an important animal pathogen widely disseminated in the environment that has also been associated with Crohn's disease in humans. Three *M. avium* subsp. *paratuberculosis* genomotypes are recognized, but genomic differences have not been fully described. To further investigate these potential differences, a 60-mer oligonucleotide microarray (designated the MAPAC array), based on the combined genomes of *M. avium* subsp. *paratuberculosis* (strain K-10) and *Mycobacterium avium* subsp. *hominissuis* (strain 104), was designed and validated. By use of a test panel of defined *M. avium* subsp. *paratuberculosis* strains, the MAPAC array was able to identify a set of large sequence polymorphisms (LSPs) diagnostic for each of the three major *M. avium* subsp. *paratuberculosis* types. *M. avium* subsp. *paratuberculosis* type II strains contained a smaller genomic complement than *M. avium* subsp. *paratuberculosis* type I and *M. avium* subsp. *paratuberculosis* type III genomotypes, which included a set of genomic regions also found in *M. avium* subsp. *hominissuis* 104. Specific PCRs for genes within LSPs that differentiated *M. avium* subsp. *paratuberculosis* types were devised and shown to accurately screen a panel ($n = 78$) of *M. avium* subsp. *paratuberculosis* strains. Analysis of insertion/deletion region INDEL12 showed deletion events causing a reduction in the complement of mycobacterial cell entry genes in *M. avium* subsp. *paratuberculosis* type II strains and significantly altering the coding of a major immunologic protein (MPT64) associated with persistence and granuloma formation. Analysis of MAPAC data also identified signal variations in several genomic regions, termed variable genomic islands (vGIs), suggestive of transient duplication/deletion events. vGIs contained significantly low GC% and were immediately flanked by insertion sequences, integrases, or short inverted repeat sequences. Quantitative PCR demonstrated that variation in vGI signals could be associated with colony growth rate and morphology.

Mycobacterium avium subsp. *paratuberculosis* is a weakly gram-positive, acid-fast bacillus causing chronic enteritis, or Johne's disease (JD), in many animal species, including primates. JD is an infectious wasting condition that develops as a consequence of chronic inflammation of the gastrointestinal tract and is an important cause of economic losses associated with farm animals (17, 22). Long-term excretion by animals with subclinical or clinical infection has led to the establishment of reservoirs in many wildlife species and extensive spread into the environment and dairy products. This exposure of humans to *M. avium* subsp. *paratuberculosis* and the findings that *M. avium* subsp. *paratuberculosis* can be detected in a significant majority of patients with Crohn's disease, a chronic enteritis of humans with striking similarities to JD, suggest the potential, although still controversial, of this organism as a zoonotic agent (2, 4, 14, 18, 28).

To fully investigate these links, it is important to accurately define *M. avium* subsp. *paratuberculosis* phylogeny. Previously, three major *M. avium* subsp. *paratuberculosis* types have been classified using pulsed-field gel electrophoresis (PFGE), IS*900* restriction fragment length polymorphism, PCR and restriction enzyme analysis of *gyrB*, denaturing gradient gel electrophoresis, and conventional culture characteristics (6, 9, 10, 16, 33, 39). These include type I (previously described as the "sheep type"), comprising pigmented and nonpigmented strains isolated from sheep in Morocco, Scotland, Iceland, South Africa, Australia, and New Zealand, strains isolated from cattle in Australia and Iceland, and some Norwegian and New Zealand caprine strains; type II (previously described as the "cattle type"), which is associated primarily with cattle but which can also be isolated from a broad range of hosts, including humans; and type III (intermediate type), which has been described for a few ovine isolates from South Africa, Canada, and Iceland and a porcine isolate from Canada, as well as caprine and bovine isolates from Spain (8). Previous comparative genomic hybridizations (CGH) between *M. avium* subsp. *paratuberculosis* strains and other related members of the *M. avium* complex (MAC) have demonstrated the presence of broad genomic differences called either genomic islands, comprising

* Corresponding author. Mailing address: Division of Cellular and Molecular Medicine, St. George's University of London, Cranmer Terrace, London SW17 0RE, United Kingdom. Phone: 44 (0)208 725 5580. Fax: 44 (0)208 725 2812. E-mail: tim.bull@sgul.ac.uk.

† Supplemental material for this article may be found at http://aem.asm.org/.

▽ Published ahead of print on 1 December 2008.

TABLE 1. Origins of *M. avium* subsp. *paratuberculosis* isolates

Strain(s)	Host breed	Origin	PFGE type
Isolates used for MAPAC array (n = 12)			
M189	Finn sheep	Scotland (central)	I pigmented
213G	Sheep	Scotland (Shetland)	I pigmented
6760B	Sheep	New Zealand	I
896	Bullfighting cattle	Spain (north central)	II
CAM20, CAM84	Guadarrama goat	Spain (central)	II
574	Murciano-Granadina goat	Spain (south central)	II
619, 841	Bullfighting cattle	Spain (south central)	III
CAM38, CAM86, CAM87	Guadarrama goat	Spain (central)	III
Additional isolates used for PCR screening (n = 66)			
21P	Sheep	Denmark (Faroe Islands)	I pigmented
208G, 235G	Sheep	Scotland (Shetland)	I pigmented
813, 940, MI05/02938-2	Bullfighting cattle	Spain (north central)	II
D206	Fallow deer	Spain (south)	II
172	Goat	Unknown	II
232, 388, 416, 417, 427, 439, 446, 456, 464, 465, 469, 474, 484, 611, 872, 915, 916, CAM19, CAM63, CAM72, CAM07, MI05/03721-2	Guadarrama goat	Spain (central)	II
51, 53, 55, 56	Holstein cattle	Spain (Balearic Islands)	II
682	Holstein cattle	Spain (central)	II
25, 27, 33, 34, 35	Holstein cattle	Spain (north)	II
10	Limousine cattle	Spain (north central)	II
1	Mouflon	Spain (north central)	II
46, 72, 78, 83, 87, 90, 94, 106, 45b, N10, N11, N21, N24, N29, N42, N64, N65, N90, N105, N109, N124	Murciano-Granadina goat	Spain (south central)	II
733	Bullfighting cattle	Spain (north central)	III
CAM40, CAM42	Guadarrama goat	Spain (central)	III

regions of contiguous genes (42) probably acquired as single units by horizontal transfer (1), or large sequence polymorphisms (LSPs) (31, 32, 35, 37). Some LSPs specifically associate with distinct *M. avium* subsp. *paratuberculosis* types and have indicated that *M. avium* subsp. *paratuberculosis* strains found predominantly in sheep are much more closely related to other members of the MAC than are the more commonly isolated *M. avium* subsp. *paratuberculosis* type II strains, suggesting that *M. avium* subsp. *paratuberculosis* type II strains have a reduced genomic complement (11, 24, 36).

This work addresses these analyses in depth with the development of a microarray that comprises optimized 60-mer oligonucleotide reporters designed to represent the gene contents of the sequenced genomes of two closely related members of the MAC, *M. avium* subsp. *paratuberculosis* K-10 and *Mycobacterium avium* subsp. *hominissuis* strain 104. We describe the use of this array (designated the MAPAC array) to characterize a range of *M. avium* subsp. *paratuberculosis* genomotypes, particularly focusing upon *M. avium* subsp. *paratuberculosis* type I and III strains from various animal hosts. The study highlights the close relation of *M. avium* subsp. *paratuberculosis* type I and III strains while showing significant genomic deletions, similarities to *M. avium* subsp. *hominissuis* 104, and variations in gene copy number of low-GC% gene regions, which we suggest may contribute to host preferences and variations in epidemiological spread observed for these *M. avium* subsp. *paratuberculosis* types.

MATERIALS AND METHODS

Mycobacterial strains. Reference strains used in this study included *M. avium* subsp. *paratuberculosis* K-10 (ATCC BAA-968) and *M. avium* subsp. *hominissuis* 104 (a kind gift from Marcel Behr, Canada). Reference strain *M. avium* subsp. *paratuberculosis* K-10 is *M. avium* subsp. *paratuberculosis* type II, originally isolated from a cow with JD (23), and *M. avium* subsp. *hominissuis* 104 is a *Mycobacterium avium* subsp. *hominissuis* serotype 4 strain originally isolated from an AIDS patient (21). *M. avium* subsp. *paratuberculosis* strains from various regions in Spain, Scotland, and Denmark (Table 1) were isolated as previously described by de Juan et al. (9) and Stevenson et al. (39). Primary cultures were incubated at 37°C for up to 10 months on Middlebrook 7H11 agar supplemented with Selectatabs (amphotericin B, polymyxin B, carbenicillin, and trimethoprim; code MS 24; MAST Laboratories, Ltd., Merseyside, United Kingdom), 10% Middlebrook oleic acid-albumin-dextrose-catalase enrichment medium (Difco, Surrey, United Kingdom), and 2 μg per ml of mycobactin J (Allied Monitor, Fayette, MO) per ml. For pigmented strains, cultures additionally contained 20% (vol/vol) heat-inactivated newborn calf serum, 2.5% (vol/vol) glycerol, and 2 mM asparagine. The study also included a sample of DNA extracted from an *M. avium* subsp. *paratuberculosis* isolate labeled 6760B (S1 restriction fragment length polymorphism profile [7]), originally isolated from a sheep in New Zealand.

DNA extraction from cultures. Cultures were grown on solid Middlebrook 7H11 medium for up to 12 weeks. For MAPAC array analysis, 10^9 cells were scraped and emulsified by passage 10 times through a 25-gauge needle into 650 μl mycobacterial lysis buffer (8.6 ml H_2O, 0.5 M EDTA [pH 8.0], 5 M NaCl, 1 M Tris-HCl, 10% sodium dodecyl sulfate [SDS], 1 mg/ml lysozyme [catalog no. L-6876; Sigma, United Kingdom]), 0.15 mg/ml proteinase K (catalog no. P-2308; Sigma, United Kingdom), and 0.5 mg/ml lipase (catalog no. L8525-1MU; Sigma, United Kingdom) and incubated at 37°C in a rotator for 1 h. Samples were added to lysing matrix B (catalog no. 6911-100; Qbiogene, United Kingdom) in 1.9-ml ribolyser reaction tubes, mechanically disrupted in a ribolysing machine (Hybaid, United Kingdom) at 6,500 rpm for 45 s, and iced for 10 min. Lysate (220 μl) was then added to 200 μl of Qiagen DNAeasy AL lysis buffer, mixed, and applied to

TABLE 2. PCR primer pairs and amplicon sizes of *M. avium* subsp. *paratuberculosis* ORFs used in this work

Region	ORF[a]	Primers (5′–3′)[b]	Size (bp)
vGI-10	Pre-16S rRNA gene	(F) TTGGCCATACCTAGCACTCC; (R) GCGCAGCGAGGTGAATTT	97
vGI-1	MAP0101	(F) GGTTACCGACTTGGTCCAGA; (R) CCCGTCAGATCCATTACGAC	238
—[c]	MAP0160	(F) ATGCTTCGCGATACTTCCAA; (R) TGAGCACCTTGTTCAAATCG	178
vGI-4	MAP0859c	(F) CCGGCGTACCTACAGACATT; (R) GAGCGATACAGGCGAAAGAC	255
vGI-4	MAP0865c	(F) CCCGATAGCTTTCCTCTCCT; (R) GATCTCAGACAGTGGCAGGTG	609
INDEL4	MAP1435	(F) TGATTGCGTTCACGTCGTC; (R) AACAGCGCATCGATCACATA	265
—	MAP2729	(F) GTGGCGGACAACGACTTC; (R) GATCTGCTCTCGCAGTTCG	216
INDEL15	MAP3584	(F) GCGTTGGATCCTTTCGTG; (R) GTCCAGGCCGTCGAGATAG	633
vGI-13	MAP3746	(F) ATGACAAGGACACCCGAAAG; (R) AGTGCAGAACTCACGCAATG	239
INDEL12	MAV_4125	(F) TCACCTGTCCAGATCAACGA; (R) CGGGATCAGCTTGAGATACC	303
INDEL12	MAV_4126	(F) GAACATGAACACCGAGGTCAC; (R) CACACGTACTCGTTGGCGTA	306

[a] Annotations are from GenBank.
[b] F, forward; R, reverse.
[c] —, not associated with vGI or LSP.

a DNAeasy column. Ethanol (100%; 200 μl) was then added and the tube sealed and mixed. Columns were washed in 500 μl Qiagen lysis buffers 1 and 2, with centrifugation at 8,000 × *g* for 1 min, and then eluted in 90 μl DNA/RNase-free H_2O overnight on the column at 4°C. DNA from single colonies with a large or small morphological appearance was prepared for PCR analysis of variable genomic islands (vGIs) by being lysed in mycobacterial lysis buffer and then extracted after ribosylation using standard phenol, phenol-chloroform, and ethanol precipitations into 50 μl DNA/RNase-free H_2O overnight. DNA for PCR screening of specific genes within LSPs was prepared from a resuspension of a loopful of colonies growing on solid media into 200 μl of sterile deionized water and heat inactivation at 100°C for 10 min and then cleared by centrifugation at 8,000 × *g* for 1 min.

Microarray design and optimization. The design strategy undertaken to generate a microarray with 60-mer oligonucleotide reporters that represented all annotated genes in *M. avium* subsp. *paratuberculosis* K-10 (GenBank accession no. NC_002944) and *M. avium* subsp. *hominissuis* 104 (GenBank accession no. NC_008595) followed the general design principles for multistrain arrays described previously (20). However, the approach taken for the MAPAC array involved an initial optimization phase to empirically select an optimal set of oligonucleotide reporters to subsequently progress to oligonucleotide synthesis and spotting using more standard robotic arraying technology (19).

For the optimization phase, multiple oligonucleotide reporters were designed in silico to represent each of the annotated genes in *M. avium* subsp. *paratuberculosis* K-10 and *M. avium* subsp. *hominissuis* 104, ensuring standard oligonucleotide design criteria of matched melting temperature and lack of secondary structures or polymeric repeats (Oxford Gene Technology [OGT], United Kingdom). Furthermore, design criteria aimed to minimize potential cross-hybridization by intrastrain paralogues while maintaining identity to interstrain orthologues. This set of 15,000 oligonucleotides, plus their associated mismatched control oligonucleotides (~15,000), were then arrayed at high density using inkjet in situ synthesis technology by OGT and hybridized with DNA from the two reference strains, namely, *M. avium* subsp. *paratuberculosis* K-10 and *M. avium* subsp. *hominissuis* 104. Based on the hybridization performance of each oligonucleotide in the inkjet in situ synthesis arrays, in terms of both relation to the mismatched control and intensity in each channel, a subset of 5,744 optimally performing oligonucleotides were selected as the final oligoset for the spotted array.

The optimal set of 60-mer oligonucleotides were synthesized (Operon Biotechnologies, Germany), supplied in 384-well plates, and resuspended at 50 mM in 50% dimethyl sulfoxide. These oligonucleotide reporters were then arrayed at high density on aminosilane-coated UltraGaps slides (Corning) by use of a MicroGrid II (BioRobotics) arraying robot. Microarrays were postprint processed according to the slide manufacturer's instructions to rehydrate, fix, and UV cross-link the oligonucleotides.

DNA labeling and microarray hybridization. DNA from the test strain and the *M. avium* subsp. *paratuberculosis* K-10 reference strain was fluorescently labeled and hybridized to the microarray using protocols described previously (12). Briefly, 1 μg of DNA was labeled by random priming with Klenow polymerase to incorporate either Cy3 or Cy5 dCTP (GE Healthcare) for the test strain or the reference strain, respectively. Equal amounts of the Cy3- and Cy5-labeled samples were copurified through a Qiagen MinElute column (Qiagen), mixed with a formamide-based hybridization solution (1× MES [morpholineethanesulfonic acid], 1 M NaCl, 20% formamide, 0.02 M EDTA, 1% Triton X-100), and denatured at 95°C for 2 min. The labeled sample was loaded on to a prehybridized (3.5× SSC [1× SSC is 0.15 M NaCl plus 0.015 M sodium citrate], 0.1% SDS, 10 mg/ml bovine serum albumin) microarray under two 22- by 22-mm LifterSlips (Erie Scientific), sealed in a humidified hybridization cassette (Corning), and hybridized overnight by immersion in a water bath at 55°C for 16 to 20 h. Slides were washed once in 400 ml 1× SSC, 0.06% SDS at 55°C for 2 min and twice in 400 ml 0.06× SSC for 2 min.

Microarray data analysis. Microarrays were scanned using an Affymetrix 428 scanner, and signal intensity data were extracted using BlueFuse for Microarrays v3.5 (BlueGnome, Cambridge, United Kingdom). The intensity data were further postprocessed using BlueFuse to exclude both controls and low-confidence data ($P < 0.1$) prior to normalization by two-dimensional Lowess (window size of 20) and median centering. Further analysis of the normalized data was undertaken using BlueFuse, GeneSpring 7.3.1 (Agilent Technologies), and Eisen Cluster (13).

Analysis methods for CGH calling to determine the genes that were present in the test strain only, present in the reference strain only, or present in both strains were undertaken as described previously for twofold and 3-standard deviation (SD) approaches (41), using a hidden Markov model for CGH calling (29), or utilizing the BlueFuse CGH calling algorithm with parameters of >2 SD for the genome, a $\log_2$ threshold of >1 or ≤1, and a minimum region size of 1.

Measures of specificity and sensitivity for each of these approaches were determined by comparison with the expected results as predicted by BLAST analysis of the oligonucleotide reporter sequences against the reference genome sequences, as described previously (41). Further cluster analysis to investigate the relatedness of strains and highlight the genomic regions of interest was undertaken using only genes called by the BlueFuse CGH algorithm either test strain specific or reference strain specific in any one of the 12 *M. avium* subsp. *paratuberculosis* strains analyzed. Clustering of log ratio data was performed in Eisen Cluster to cluster arrays using only a standard, uncentered Pearson correlation by average linkage, as the genes were maintained in genome order.

Genes that fell within a >1.5 or <2 $\log_2$ threshold increase or decrease relative to the *M. avium* subsp. *paratuberculosis* K-10 reference normalized standard and were contiguous in the genome were flagged as belonging to a vGI.

PCR. PCR primers (AltaBioscience, United Kingdom) were designed using Primer 3 software (http://biotools.umassmed.edu/bioapps/primer3_www.cgi) to specifically amplify open reading frames (ORFs) in LSP and vGI gene loci (Table 2). PCR was carried out using an Expand high-fidelity PCR system (Roche Diagnostics, Germany). Each reaction was performed with a 50-μl volume, containing 5 μl of DNA sample and 1× Expand HiFiPLUS reaction buffer containing 1.5 mM $MgCl_2$, 0.200 mM PCR nucleotide mix PCR grade, upstream and downstream primers (2 μM each), 5 μl of dimethyl sulfoxide (Sigma, United Kingdom), and 2.5 U of Expand HiFiPLUS enzyme blend, under the following conditions: denaturation at 94°C for 3 min followed by 35 cycles of denaturation at 94°C for 30 s, annealing at 58°C for 45 s, and extension at 72°C for 1 min 30 s, with a final cycle of extension at 72°C for 5 min.

Quantitative PCR (qPCR) against vGI-associated genes and gene controls for normalization was performed in duplicate in two separate experiments (see Table S1 in the supplemental material) using a Power SYBR green qPCR kit (ABgene, United Kingdom) according to the manufacturer's specifications with a Stratagene MX3000P instrument (Stratagene, United Kingdom). Estimates of

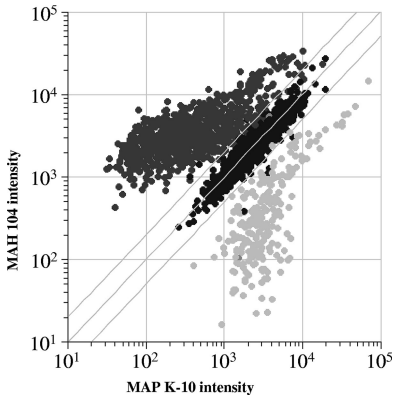

FIG. 1. Microarray data for validation hybridization comparing the two sequenced reference strains, using *M. avium* subsp. *hominissuis* 104 as the test strain and *M. avium* subsp. *paratuberculosis* K-10 as the reference strain per other strain comparisons. Scatter plots show the signal intensities for the test (*y* axis) versus the reference (*x* axis) strain channels. Data points are colored according to the BLAST prediction based on the sequence: black, predicted to be present in both the test and reference strains; light gray, predicted to be present in the test strain only; dark gray, predicted to be present in the reference strain only. Diagonal lines represent twofold cutoffs applied to each strain for each of the analysis methods used. MAH, *M. avium* subsp. *hominissuis*; MAP, *M. avium* subsp. *paratuberculosis*.

the copy number for each gene were made using calibration curves obtained for each PCR primer pair against a dilution curve of *M. avium* subsp. *paratuberculosis* K-10 reference DNA using MxPro software (Stratagene, United Kingdom). The estimated total sample copy numbers determined for each sample were initially normalized against the estimated total copy numbers of MAP0160. qPCR from MAP0160 was not available on all colonies from one experiment; therefore, MAP0101 was used to normalize samples in this case. To decrease any bias introduced by variations in amplification efficiencies between these normalizing genes, the final increases/decreases were calculated using the averages of MAP0101 and MAP0160 results from both experiments.

Microarray data accession numbers. Fully annotated microarray data have been deposited in BμG@Sbase (accession no. A-BUGS-35 and E-BUGS-69) (http://bugs.sgul.ac.uk/E-BUGS-35 and http://bugs.sgul.ac.uk/E-BUGS-69, respectively) and also ArrayExpress (accession no. A-BUGS-35 and E-BUGS-69).

RESULTS

MAPAC microarray validation. An evaluation of the MAPAC microarray performance was made by hybridizing labeled DNA from the sequenced reference strains *M. avium* subsp. *paratuberculosis* K-10 and *M. avium* subsp. *hominissuis* 104 (Fig. 1). Comparison of these hybridization data with BLAST predictions indicated that the array was correctly identifying genes specific to *M. avium* subsp. *paratuberculosis* K-10 or *M. avium* subsp. *hominissuis* 104 and also genes shared between *M. avium* subsp. *paratuberculosis* K-10 and *M. avium* subsp. *hominissuis* 104. Measures of sensitivity and specificity, using the various analysis approaches to identify genes present or absent/highly divergent in *M. avium* subsp. *hominissuis* 104 compared to *M. avium* subsp. *paratuberculosis* K-10, supported the validation of the array using the twofold (sensitivity of 98%, specificity of 98%), 3-SD (sensitivity of 98%, specificity of 98%), hidden Markov model (sensitivity of 91%, specificity of 96%), or BlueFuse CGH (sensitivity of 98%, specificity of 99%) approach.

The BlueFuse CGH calling protocol was established as providing a reliable and automated call on strain-specific genes for the two reference strains, with the best balance of false positives (2%) to false negatives (1%), and therefore this method was chosen for the analysis of all other strains. A subset of genes that were called either test strain specific or reference strain specific in any one of the test strains was selected. This subset of genes represented the genes of interest that would include genomic differences between strains and so was subjected to clustering. A summary of the clustering results and genomic loci of interest are presented in Table 3, with a complete clustering tree provided in Fig. S1 in the supplemental material. A full set of hybridization ratios with predicted gene functions for each gene are supplied in Table S2 in the supplemental material.

***M. avium* subsp. *hominissuis* 104 genomic loci present in *M. avium* subsp. *paratuberculosis* type I and type III strains.** All of the *M. avium* subsp. *paratuberculosis* type I and type III strains but none of the *M. avium* subsp. *paratuberculosis* type II strains, including the reference strain *M. avium* subsp. *paratuberculosis* K-10, showed significant differences in hybridization when analyzed by microarray, suggesting the presence of 89 ORFs also present in the *M. avium* subsp. *hominissuis* 104 genome (Table 3). These included three single ORFs (insertion/deletion 1 [INDEL1], or MAV_0339 [*tetR* regulator]; INDEL8, or MAV_2254 [function unknown]; and INDEL9, or MAV_2223 [IS*6120*]) and six LSPs (INDEL3, or MAV_3258 to MAV_3270 [previously described as MAV17 {42}]; INDEL5, or MAV_2978 to MAV_2998 [previously described as MAV14 {42}]; INDEL10, or MAV_1975 to MAV_2008 [previously described as MAV7 {42}]; INDEL12, or MAV_4125 to MAV_4130 [previously described as MAV21 {42}]; INDEL14, or MAV_4351 to MAV_4353 [dioxygenase]; and INDEL16, or MAV_5225 to MAV_5243 [previously described as MAV24 {42}]) containing prevalent predicted functions involving lipid metabolism (31). Full putative-function lists are supplied in Table S2 in the supplemental material.

Deletion of *M. avium* subsp. *paratuberculosis* genomic loci associated with *M. avium* subsp. *paratuberculosis* type I and type III strains. All *M. avium* subsp. *paratuberculosis* type I and type III strains arrayed by MAPAC showed a significant decrease in hybridization relative to that for *M. avium* subsp. *paratuberculosis* K-10 in a total of 26 ORFs (Table 3). These included INDEL2, or MAV_0775 (an ORF not called in the *M. avium* subsp. *paratuberculosis* annotation but positioned between MAP0660 and MAP0661); INDEL6, or MAP1484 to MAP1491; and INDEL7, or MAP1728c to MAP1744 (previously described as LSP locus S2 [24]). All *M. avium* subsp. *paratuberculosis* type I strains had additional deletions of INDEL11, or MAP2704 (hemolysin III like), and decreased signals to INDEL13, or MAP3460c (a transposase with eight similar copies in *M. avium* subsp. *paratuberculosis* K-10). All *M. avium* subsp. *paratuberculosis* type III strains had additional deletions of INDEL4, or MAP1433c to MAP1438c (lipid metabolism), and INDEL15, or MAP3584 (alkanesulfonate monooxygenase). Each of these deleted ORFs was present in *M. avium* subsp. *hominissuis* 104. All of the strains tested contained MAP2325, which has previously been reported as deleted from some *M. avium* subsp. *paratuberculosis* type I sheep strains isolated in Australia (24).

Screening of *M. avium* subsp. *paratuberculosis* strain panel for INDELs by PCR. To confirm INDELs described by the

TABLE 3. Summary of significant signal divergences from multiple probes in LSPs and vGIs in *M. avium* subsp. *paratuberculosis* types I, II, and III and *M. avium* subsp. *hominissuis* 104 compared with *M. avium* subsp. *paratuberculosis* K-10

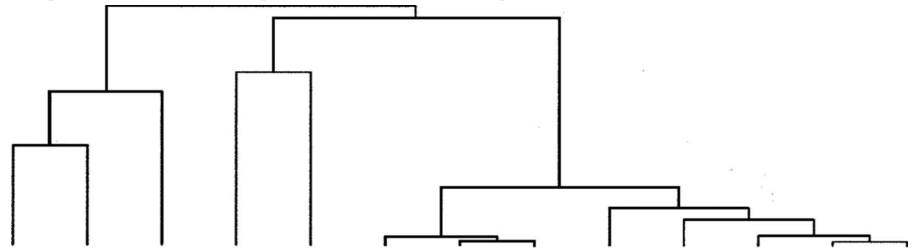

Region[a]	Locus tag(s)	Signal divergence[b]											
		M. avium subsp. *hominissuis* 104	*M. avium* subsp. *paratuberculosis* type II strains				*M. avium* subsp. *paratuberculosis* type I strains			*M. avium* subsp. *paratuberculosis* type III strains				
			CAM84	896	CAM20	574	6760B	M189	213G	619	CAM87	CAM86	CAM38	841
vGI-1a	MAP0071 to MAP0093	.	.	.	.	V−	.	.	.	.	+	V+	.	.
vGI-1b	MAP0094 to MAP0103c	−−	.	.	.	.	V−	V−	.	.	+	V+	.	.
vGI-2	MAP0281 to MAP0283c	−−	.	.	.	.	V−	V−	.	.	+	V+	.	.
INDEL1	MAV_0339	+	.	.	.	.	++	++	++	++	++	++	++	++
INDEL2 (MAV4)	MAV_0775 (MAP0660 to MAP0661)	.	.	.	.	+	−	−	−−	−	−	−	−	−
vGI-3	MAP0758 to MAP0774c	.	.	.	.	.	.	V−	.	.	+	V+	.	.
vGI-4	MAP0852 to MAP0866	−−	V−	.	.	.	V−	V−	.	.	+	V+	.	.
vGI-5	MAP1231 to MAP1236c	−	.	.	.	.	V−	V−	.	V+	+	V+	.	.
INDEL3 (MAV17)	MAV_3258 to MAV_3270	++	.	.	.	.	++	++	++	++	++	++	++	++
INDEL4	MAP1433c to MAP1438c	.	.	.	.	.	.	.	.	−−	−−	−−	−−	−−
INDEL5 (MAV14)	MAV_2978 to MAV_2998	++	.	.	.	.	++	++	++	++	++	++	++	++
INDEL6	MAP1484 to MAP1491	.	.	.	.	.	−−	−−	−−	−−	−−	−−	−−	−−
vGI-6	MAP1631c to MAP1637c	−−	.	.	.	.	.	V−	V−	V+	+	V+	.	.
vGI-7	MAP1720 to MAP1727	−−	.	.	.	.	.	V−	V−	V+	V+	V+	.	.
INDEL7 (S2)	MAP1728c to MAP1744	.	.	.	.	.	−−	−−	−−	−−	−−	−−	−−	−−
INDEL8 (MAV10)	MAV_2254	++	.	.	.	.	++	++	++	++	++	++	++	++
INDEL9	MAV_2223	++	.	.	.	.	++	++	++	++	++	++	++	++
vGI-8	MAP2025 to MAP2031	−	.	.	.	.	.	V−	V−	V+	+	V+	.	.
vGI-9	MAP2151 to MAP2157	−−	.	.	.	V+	.	V−	V−	V+	+	V+	.	.
INDEL 10 (MAV7)	MAV_1975 to MAV_2008	++	.	.	.	.	++	++	++	++	++	++	++	++
vGI-10	MAP2443 to MAP2457c	.	.	.	.	.	.	.	.	V+	+	V+	.	.
vGI-11	MAP2523c to MAP2529	.	.	.	.	.	.	V−	.	V+	+	V+	.	.
INDEL11	MAP2704	.	.	.	.	.	−	−	−−	.	.	.	.	.
vGI-12	MAP2767c to MAP2769c	−−	.	.	.	.	.	V−	V−	.	+	V+	.	.
INDEL12 (MAV21)	MAV_4125 to MAV_4130	++	.	.	.	.	++	++	++	++	++	++	++	++
INDEL13	MAP3460c	−	.	.	.	.	−	−	−	.	.	.	.	.
INDEL14	MAV_4351 to MAV_4353	++	.	.	.	.	++	++	++	++	++	++	++	++
INDEL15	MAP3584	.	.	.	.	.	.	.	.	−	−	−	−	−
vGI-13	MAP3730 to MAP3747c	−−	.	.	.	.	.	V−	.	V+	+	V+	.	.
vGI-14	MAP3749 to MAP3770c	−−	.	.	.	.	.	V−	.	V+	+	V+	.	.
vGI-15	MAP3815 to MAP3818	−−	.	.	.	.	.	.	.	.	+	V+	.	.
vGI-16	MAP4266 to MAP4267	−−	.	.	.	.	.	.	.	.	+	.	.	.
INDEL16 (MAV24)	MAV_5225 to MAV_5243	++	.	.	.	.	++	++	++	++	++	++	++	++

[a] Nomenclature of previously annotated LSPs associated with INDELs is given in parentheses.

[b] −, signal >2- and <5-fold less than that for K-10; −−, signal >5-fold less than that for K-10; ., signal >1.5-fold less than and <1.5-fold greater than that for K-10; V−, signal >1.5- and <2-fold less than that for K-10; +, signal >2-fold and <5-fold greater than that for K-10; ++, signal >5-fold greater than that for K-10; V+, signal >1.5- and <2-fold greater than that for K-10.

microarray, we used specific PCRs for INDEL4, INDEL12, and INDEL15 (Table 2) to screen 66 *M. avium* subsp. *paratuberculosis* strains recovered from different geographic areas and hosts in Spain, Scotland, and Denmark that had previously been typed by PFGE (Table 1) and confirmed those previously submitted for microarray analysis ($n = 12$). PCRs for INDEL15 (MAP3584) were positive for all *M. avium* subsp. *paratuberculosis* type I strains ($n = 6$) and *M. avium* subsp. *paratuberculosis* type II strains ($n = 64$) but negative for all *M. avium* subsp. *paratuberculosis* type III strains ($n = 8$).

TABLE 4. Summary of specific *M. avium* subsp. *paratuberculosis* gene PCRs performed with DNA extracted from *M. avium* subsp. *paratuberculosis* strains isolated from various hosts and locations

Type	Host(s) (no. of strains)	Presence (+) or absence (−) of locus tag:				
		MAP3584	MAP1435	MAV_4125	MAV_4126	MAP865
I	Sheep (5)	+	+	+	+	+
	Sheep (1)	+	−	+	−	+
II	Cattle (15), goat (47), fallow deer (1), mouflon (1)	+	+	−	−	+
III	Cattle (3), goat (5)	−	−	+	+	+

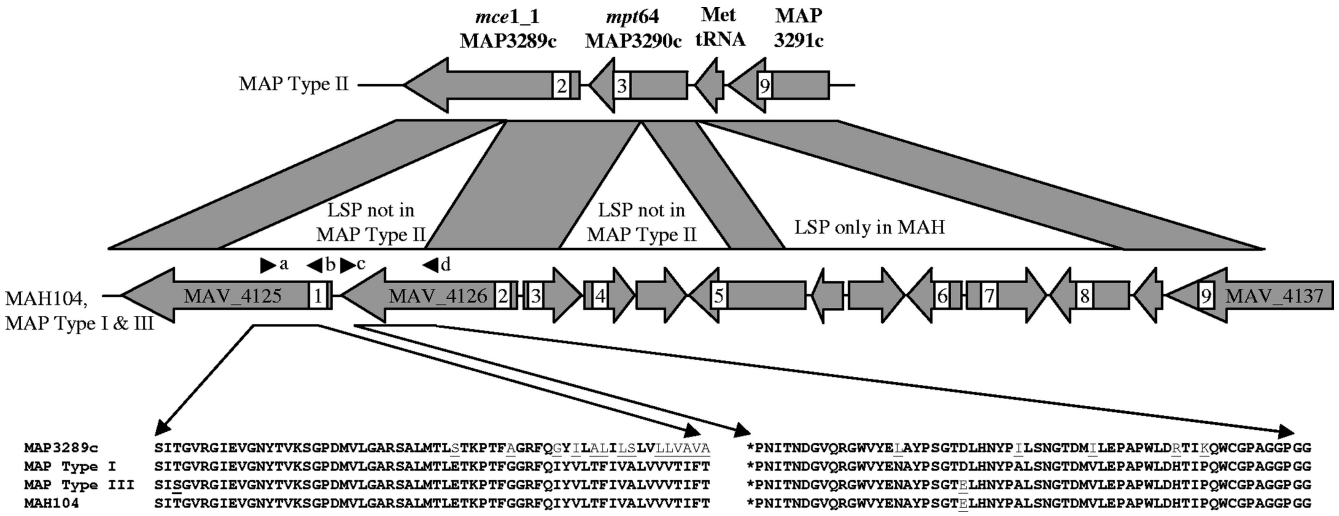

FIG. 2. Diagrammatic genomic alignment of the *M. avium* subsp. *paratuberculosis* type II (MAP3289c to MAP3291c) region against *M. avium* subsp. *paratuberculosis* type I and III strains and *M. avium* subsp. *hominissuis* 104 (MAV_4125 to MAV_4137), showing homologies (gray) and locations of LSPs that have generated the *mce1_1* gene by fusing sections of MAV_4125 and MAV_4126 and the *mpt64* gene by fusing sections of MAV_4130 and the complement of MAV_4127. The approximate positions of gene probes 1 to 9 used in the MAPAC array are indicated in white boxes. The positions of PCR primer pairs used for detection of MAV_4125 (a and b) and MAV_4126 (c and d) are also shown. Sequence differences (underlined) observed in the MAV_4126 and MAV_4127 genes of *M. avium* subsp. *paratuberculosis* and *M. avium* subsp. *hominissuis* 104 obtained from PCR amplicons generated using primers a and d are indicated and aligned against MAP3289c obtained from the *M. avium* subsp. *paratuberculosis* K-10 genome sequence. MAH, *M. avium* subsp. *hominissuis*; MAP, *M. avium* subsp. *paratuberculosis*.

INDEL12 (MAV_4125) PCRs were positive for all *M. avium* subsp. *paratuberculosis* type I and type III strains but negative for all *M. avium* subsp. *paratuberculosis* type II strains. INDEL12 (MAV_4126) PCRs were positive for all *M. avium* subsp. *paratuberculosis* type III strains and type I pigmented strains but negative for all other strains. PCRs for INDEL4 (MAP1435) were positive for all *M. avium* subsp. *paratuberculosis* type I and type II strains but negative for all *M. avium* subsp. *paratuberculosis* type III strains (Table 4).

LSP INDEL12 sequence analysis. MAPAC results for INDEL12 were not fully consistent with previously described array data covering this region (32). We therefore performed sequencing on PCR products amplified from *M. avium* subsp. *paratuberculosis* type I strain M189 (EMBL accession no. FM199950) and *M. avium* subsp. *paratuberculosis* type III strain CAM86 (EMBL accession no. FM199949) with primers specific to MAV_4125 and MAV_4126 located within INDEL12 and compared these with the *M. avium* subsp. *paratuberculosis* K-10 and *M. avium* subsp. *hominissuis* 104 reference genomes (Fig. 2). This showed that in *M. avium* subsp. *paratuberculosis* type II strains, as a consequence of a small internal deletion, a fusion of the MAV_4125 C terminus and the MAV_4126 N terminus resulted in a new ORF (MAP3289c), while *M. avium* subsp. *paratuberculosis* type I strain M189 and *M. avium* subsp. *paratuberculosis* type III strain CAM86 retained both genes with 99% homology to *M. avium* subsp. *hominissuis* 104 gene sequences but each containing nonsynonymous sequence divergences specific to each *M. avium* subsp. *paratuberculosis* type. MAV_4125 and MAV_4126 are both homologues of *M. avium* subsp. *paratuberculosis* mycobacterial cell entry genes, which demonstrates that *M. avium* subsp. *paratuberculosis* type II strains contain a decreased complement of these important virulence determinants. In addition, the immediately adjacent sequence alignments show a similar small deletion that has resulted in the replacement of 30% of the C terminus of the *M. avium* subsp. *paratuberculosis* type II *mpt64* gene (MAP3290c) compared to its homologue MAV_4130 present in both *M. avium* subsp. *paratuberculosis* type I and type III strains and *M. avium* subsp. *hominissuis* 104.

vGI analysis. MAPAC array data revealed 16 vGIs totaling 138 kb (see Table S2 in the supplemental material) that were present and variable in type I and type III isolates but present but not variable in type II isolates. Ten vGIs were present within the *M. avium* subsp. *paratuberculosis* K-10 reference genome and absent from the *M. avium* subsp. *hominissuis* 104 genome, thus being partially or completely inclusive of *M. avium* subsp. *paratuberculosis* LSPs. A comparison of GC% contents of vGIs against those of LSPs not associated with vGIs showed that the vGI group had a GC% significantly ($P = 0.0005$; Mann-Whitney) lower than that of the LSP group. In addition, 80% of vGIs were immediately bounded by short inverted repeats and 40% were immediately bounded by or contained integrase proteins and transpositional elements, including IS*900*, IS*1311*, IS*1610*, and IS*1110* (Table 5).

qPCR amplifications designed to amplify MAP0101 within vGI-1, MAP0859c within vGI-4, MAP3746 within vGI-13, and a pre-16S rRNA ribosomal gene sequence within vGI-10 were performed on DNA extractions from single colonies of *M. avium* subsp. *paratuberculosis* type II and type III strains to measure variations in gene copy number. qPCR threshold cycle signal values were converted to copy number estimates using calibration curves against DNA from reference strain *M. avium* subsp. *paratuberculosis* K-10 for each gene tested. The copy number estimate for each of the tested genes was then

TABLE 5. Positions, nomenclature, and GC% of *M. avium* subsp. *paratuberculosis* K-10 LSPs and vGIs with associated transposable elements not present in *M. avium* subsp. *hominissuis* 104

LSP name[a]	LSP locus tag(s)	vGI name	vGI locus tag(s)	GC%	Associated transposition element(s)	Associated short inverted repeat sequence	Associated short inverted repeat location(s)
		vGI-1a	MAP0071 to MAP0093	65.84			
MAP1, or LSPp1	MAP0092 to MAP0108	vGI-1b	MAP0094 to MAP0103c	63.89	MAP0104 (IS*1311*)	CGGTGATCCGCCG	MAP092 to MAP0103c/ MAP0104
MAP2, or LSPp2	MAP0282c to MAP0284c	vGI-2	MAP0281 to MAP0283c	60.57		CACGCCGACGCC	MAP0280 to MAP0284c
MAP3, or LSPp3	MAP0387 to MAP0389			65.73			
		vGI-3	MAP0758 to MAP0774c	65.81		CGAGGTCGTCCGCT	MAP0758 to MAP0774c
MAP4, or LSPp4	MAP0850c to MAP0866	vGI-4	MAP0852 to MAP0866	59.91	MAP0849 (IS*1311*), MAP0850 (ISMav2), MAP0866 (integrase)	CGGACGGGCGG	MAP0850 to MAP0866
MAP5, or LSPp5	MAP0956 to MAP0967			69.61		GCGCAGCGCGTCG	MAP0957 to MAP0967c
MAP6, or LSPp6	MAP1231 to MAP1237c	vGI-5	MAP1231 to MAP1236c	58.60		TGGGGCTACGC	MAP1230 to MAP1236
MAP7, or LSPp7	MAP1344 to MAP1349c			67.32		GGCGCTGACGCTG	MAP1344 to MAP1349
MAP8, or LSPp8	MAP1631c to MAP1638c	vGI-6	MAP1631c to MAP1637c	61.63		GCGGCGGGACGAA	MAP1630 to MAP1637c
MAP9, or LSPp9	MAP1718c to MAP1727	vGI-7	MAP1720 to MAP1727	65.34	MAP1722 (IS*900*)		
MAP11, or LSPp10	MAP2026 to MAP2029c	vGI-8	MAP2025c to MAP2031c	65.80	MAP2034c (IS*900*)	GCCGCGCGGGCG	MAP2025c to MAP2031c
						GACCAAGGCGGC	MAP2026 to MAP2032c
MAP12, or LSPp11	MAP2148 to MAP2158	vGI-9	MAP2151 to MAP2157	58.99	MAP2150 (IS*1311*), MAP2155 (IS*1610*), MAP2157 (IS*900*)	GCGGCGCCGCCGG	MAP2150 to MAP2157
MAP13, or LSPp12	MAP2178 to MAP2196			66.93		GTCCTCGACGG	MAP2178 to MAP2196
MAP14, or LSPp13	MAP2751 to MAP2769c			67.46		TGGGCGGCCTGG	MAP2752 to MAP2769/ MAP2770
		vGI-10	MAP2443 to MAP2457c	64.17	MAP2444c (IS*900*)	CCGGGATCGCCG	MAP2443 to MAP2457c
		vGI-11	MAP2523c to MAP2529	64.43			
		vGI-12	MAP2767c to MAP2769c	62.02	MAP2769 (integrase)	CGCGGCAACCG	MAP2767c to MAP2769c
MAP16, or LSPp14	MAP3721 to MAP3764	vGI-13	MAP3730 to MAP3747c	64.91	MAP3748 (IS*1110*)	CGATGTGCTGCT	MAP3730 to MAP3747c
		vGI-14	MAP3749 to MAP3770c	61.15	MAP3748 (IS*1110*), MAP3759c (IS*1311*)	TTTTCAATAAGCGT	MAP3747c/MAP3748 to MAP3969/MAP3770c
MAP16, or LSPp15	MAP3770 to MAP3776c			65.00			
LSPp16	MAP3814 to MAP3818	vGI-15	MAP3815 to MAP3818	60.74	MAP3814c (IS*900* like)	CAGGAAGCGGG	MAP3814 to MAP3819
MAP17, or LSPp17	MAP4266 to MAP4270	vGI-16	MAP4266 to MAP4267	62.20		AGACGCAAAAGCC CCCG	MAP4265 to MAP4266
						TGCGGCAGGCG	MAP4266 to MAP4271
MAP18	MAP4326c to MAP4328c			66.06			

[a] Nomenclature as described in previous studies (32, 35, 42).

normalized against average copy number estimates obtained for MAP0101 and MAP0160 (assumed to be present in single copies in each genome) to provide ratios between copy number estimates (Table 6). Ratios of MAP2729 in vaccine strain II (a known duplication in this strain) illustrated that a fivefold increase could be indicative of duplication using this analysis. All other genes in each of the *M. avium* subsp. *paratuberculosis* type II colonies tested showed no significant change in copy number above that of the *M. avium* subsp. *paratuberculosis* K-10 reference strain. MAP2729 and MAP0859c showed a trend toward an increase in the ratio of *M. avium* subsp. *paratuberculosis* type III isolates but this was not statistically significant from that of *M. avium* subsp. *paratuberculosis* type II isolates. However, both pre-16S rRNA gene and MAP3746 qPCRs showed modest increases ($P = 0.037$) between *M. avium* subsp. *paratuberculosis* type III and type II strains with pre-16S rRNA from a large colony of the *M. avium* subsp. *paratuberculosis* type III strain CAM86, exhibiting a fourfold increase which was not significantly sufficient to be called a duplication.

A comparison of large and small colonies picked from the same culture slant showed no significant difference between ratios in any of the tested genes in two *M. avium* subsp. *paratuberculosis* type II strains. However, there were significant increases (two- to threefold) from genes within vGI-4 (represented by MAP0859c) and vGI-13 (represented by MAP3746) when comparing small and large colonies of *M. avium* subsp. *paratuberculosis* type III CAM86 strains (Table 6).

TABLE 6. Ratios of qPCR-derived copy number estimates of genes from *M. avium* subsp. *paratuberculosis* type II and type III strains

Strain	Ratio (*n*-fold) of copy no.[a]					
	Pre-16S rRNA gene	MAP3746	MAP2729	MAP0859c	MAP0101	MAP0160
Type III strains						
841	2.1	2.52	1.87	1.88	1.09	0.92
CAM86 large colony	4.09	1.9	1.51	1.35	0.82	1.28
CAM86 small colony	3.27	0.87	0.66	0.61	0.75	1.49
CAM87	1.65	1.41	0.52	0.86	0.78	1.39
Type II strains						
456 large colony	0.93	1.06	0.71	0.74	0.88	1.15
456 small colony	1.32	1.12	0.67	1.01	1	NT[b]
CAM63 large colony	1	1	1	1	1	1
CAM63 small colony	0.91	1	1.31	1.1	1	NT
Vaccine II	1.09	1.24	5.16	1.65	1.02	0.98
K-10	1	1	1	1	1	1

[a] Significance between *M. avium* subsp. *paratuberculosis* type II and type III strains for the pre-16S rRNA gene and MAP3746 showed a *P* value of 0.037; all other values were nonsignificant.
[b] NT, not tested.

DISCUSSION

This work describes the design, validation, and application of the MAPAC pan-genome microarray comprised of optimized oligonucleotide reporters to generate a specific signal for each of the shared and unique ORFs present in the *M. avium* subsp. *hominissuis* 104 and *M. avium* subsp. *paratuberculosis* K-10 genomes. Validation performed using reference strain genome preparations demonstrated excellent sensitivity and specificity in determining known genomic differences with low false-positive and false-negative rates.

The MAPAC array was applied in this study to characterize the genomes of a representative panel of 12 *M. avium* subsp. *paratuberculosis* strains, including types I, II, and III. A comparison of MAPAC results with other published arrays (24, 32, 35, 42) confirmed previously annotated LSPs within *M. avium* subsp. *paratuberculosis* K-10 and *M. avium* subsp. *hominissuis* 104 genomes. Minor differences were observed at the very ends of some LSPs, and these could be explained by variations in the locations of reporters within ORFs during array designs. Additional small divergences not reported by other array formats were also detected. Consistent genetic features were found in each group of strains within an *M. avium* subsp. *paratuberculosis* type. Comparative array data demonstrated that all *M. avium* subsp. *paratuberculosis* type I ($n = 6$) and type III ($n = 8$) strains tested contained nine separate genomic loci (62 ORFs) not present or deleted in *M. avium* subsp. *paratuberculosis* type II strains but highly homologous in base sequence and gene order to the reference genome of *M. avium* subsp. *hominissuis* 104. These included the insertion sequence IS*6120* (MAV_2223), a set of *mce* genes (MAV_4125 to MAV_4130, MAV_4351, and MAV_4353) involved in taurine metabolism, and the previously described LSPs MAV17 (MAV_3258 to MAV_3270), MAV14 (MAV_2978 to MAV_2998), and MAV24 (MAV_5225 to MAV_5243) (31, 37, 42).

All *M. avium* subsp. *paratuberculosis* type I pigmented strains had deletions of MAP2704, a hemolysin III homologue (25) associated with virulence and invasion of the MAC in human disease. They also lacked MAP3460c, a transposase, possibly reflecting a variation in copy number of this gene present in nine similar copies in the *M. avium* subsp. *paratuberculosis* K-10 genome. All *M. avium* subsp. *paratuberculosis* type III strains contained a deletion of the *M. avium* subsp. *paratuberculosis*-specific region MAP1433c to MAP1438c, which has putative functions suggesting alterations in lipid and fatty acid metabolism, and also a deletion of MAP3584, an alkanesulfonate monooxygenase putatively involved in sulfur metabolism. Differences in *M. avium* subsp. *paratuberculosis* genomotypes within INDEL4, INDEL12, and INDEL15 were confirmed by using PCRs designed to screen for these characteristic deletions and *M. avium* subsp. *hominissuis* 104 homologous loci within *M. avium* subsp. *paratuberculosis* types I, II, and III. These results were fully consistent with MAPAC data from a panel of 66 *M. avium* subsp. *paratuberculosis* strains, including 60 *M. avium* subsp. *paratuberculosis* type II cattle isolates, 3 *M. avium* subsp. *paratuberculosis* type I isolates from sheep in Scotland and Denmark, and 3 *M. avium* subsp. *paratuberculosis* type III intermediate strains from Spanish goats and bullfighting cattle.

In other mycobacterial species, such as the *Mycobacterium tuberculosis* group, phylogenetic diversity and variability of host specificity or pathogenesis can be attributed mostly to gene deletions or the creation of pseudogenes via mutations. Comparison of our results with previous studies confirmed that all *M. avium* subsp. *paratuberculosis* types contain the *Mycobacterium avium* subsp. *avium* serotype 2 gene cassette but have diverged into two major phylogenetic branches originating from an IS*900*-positive progenitor. The *M. avium* subsp. *paratuberculosis* type II genomotype has undergone a series of major genomic deletion events which at some point in the fairly recent past has had a rapid worldwide distribution and then diverged further through more limited deletions of single genes, transposition events, and genomic transformations that may have been fixed as a result of geographical enclosures. *M. avium* subsp. *paratuberculosis* type I and type III strains form separate phylogenies that appear to have retained much of the *M. avium* subsp. *avium* serotype 2 progenitor genome but sim-

ilarly are becoming more diverse as a result of rearrangements and separate single gene deletions. The design of the MAPAC array was such that it incorporated both *M. avium* subsp. *hominissuis* 104 and *M. avium* subsp. *paratuberculosis* K-10 genomes and by definition therefore could look for deletions only within this combined complement. Additional unknown genomic regions (not in the reference genomes) could therefore theoretically exist in some of these tested strains and would not be detected by our array. Further full-genome sequencing of more *M. avium* subsp. *paratuberculosis* strains is required to resolve this issue.

There appears to be a trend, but not an exclusivity of host preference, between some *M. avium* subsp. *paratuberculosis* types in particular areas. In this study, we report on *M. avium* subsp. *paratuberculosis* type III isolates in Spain that have frequently been isolated from goats and are the most predominant cause of *M. avium* subsp. *paratuberculosis* infection in cattle bred specifically for bullfighting. *M. avium* subsp. *paratuberculosis* type I pigmented strains are isolated predominantly from sheep and appear to be geographically restricted, while *M. avium* subsp. *paratuberculosis* type II strains are predominant in cattle and deer and present in many other animal species. Host-pathogen interplay could also contribute to conditions likely to promote host-specific adaptations through gene redundancies, which, while not creating host exclusivity, may positively select for genomotypes and thus phenotypes associated with discrete animal groups. This is reflected in the unique pigmentation or very slowly growing phenotypes characteristic of particular *M. avium* subsp. *paratuberculosis* type I strains and the different pathways of host intracellular signaling induced between *M. avium* subsp. *paratuberculosis* type I and type II strains during macrophage processing (26).

Of particular interest was the presence in *M. avium* subsp. *paratuberculosis* type I and type III strains of a pair of mycobacterial cell entry genes (*mce*, MAV_4125 and MAV_4126). In *M. avium* subsp. *paratuberculosis* type II strains, as a consequence of a small internal deletion, these appear to have gone through a process that has resulted in combining the C terminus of MAV_4125 and the N terminus of MAV_4126 to form a new *mce* gene (MAP3289c) with 87 to 89% identity. Using specific PCR, we have demonstrated that *M. avium* subsp. *paratuberculosis* type I pigmented and *M. avium* subsp. *paratuberculosis* type III strains contain both *mce* gene homologues but that *M. avium* subsp. *paratuberculosis* type II strains have only MAP3289c. The precise mechanism of the *mce* gene function is not fully established; however, the loss of *mce* regions in other pathogenic mycobacteria can profoundly affect virulence by decreasing the initiation of infection through cell entry (38) and important pathogenic mechanisms, such as granuloma formation (15). In the *M. avium* subsp. *paratuberculosis* type II K-10 reference genome, *mce* genes occur in seven separate clusters containing 6 to 10 ORFs (5). MAP3289c has 94% identity to *mce1A* (MAP3604) from the *mce1* cluster. MAP3604 is unique as it is the only *mce* gene homologue that is not associated with an *mce* gene cluster located immediately downstream, suggesting that this may be an ancillary gene copy. Differences in *mce* gene complement have previously been demonstrated for other members of the MAC (32) and have been proposed as important factors in defining variations in host pathogenesis. This work now shows that *M. avium* subsp. *paratuberculosis* types can also be defined through their *mce* complement and suggests that *mce* gene redundancy may be an important process in defining phenotypic differences between *M. avium* subsp. *paratuberculosis* types.

In addition, it is shown that an immediately adjacent deletion event in this genomic region has removed a series of small ORFs (MAV_4127 to MAV_4129) in *M. avium* subsp. *paratuberculosis* type II strains but not *M. avium* subsp. *paratuberculosis* type I or type III strains. This has resulted in a fusion of the N terminus of MAV_4130 with the complementary sequence of MAV_4126 and created an *M. avium* subsp. *paratuberculosis* type II-specific gene, MPT64 (MAP3290). The homologue of MAV_4130 in *M. tuberculosis* (Rv1980c) is a major immunogenic protein associated with mycobacterial persistence through the inhibition of apoptosis in multinucleated giant cells during granuloma formation (27). The replacement of 30% of MAV_4130, represented as MAP3290 in *M. avium* subsp. *paratuberculosis* type II strains, could therefore be a significant determinant in diverse mechanisms of pathogenesis and host persistence associated with infections involving this genomotype.

In some of the strains tested in this study, the MAPAC array was sufficiently sensitive to detect clusters of genes with significantly altered ratios which were consistently close to the duplication or deletion threshold as determined by analysis based on the distribution of the complete genome data set. These could be grouped into 16 regions of consecutive genes, described here as vGIs. Bioinformatic analysis revealed that vGIs corresponded closely to *M. avium* subsp. *paratuberculosis* LSPs previously described as conserved in all *M. avium* subsp. *paratuberculosis* isolates and contained a significantly lower GC% content than LSPs not associated with vGIs ($P = 0.0005$). vGIs were not detected within the *M. avium* subsp. *paratuberculosis* K-10 reference strain and were observed only rarely in the *M. avium* subsp. *paratuberculosis* type II strains tested but were frequently partially elevated (suggesting duplication) in the majority of *M. avium* subsp. *paratuberculosis* type III strains and decreased (suggesting depletion) in type I strains. vGI-5 (MAP1231 to MAP1237) forms part of a previously described genomic region associated with the emergence of rough- and smooth-colony forms of *M. avium* subsp. *avium* generated through homologous recombinatory events (3). Other vGI regions comprise a diverse group of genes associated with virulence and survival, including a set of *mce* genes (vGI-3, or MAP0758 to MAP0774c); part of the 38-kDa-siderophore, low-GC% island (vGI-13, or MAP3730 to MAP3747c; vGI-14, or MAP3749 to MAP3758c) (40); the virulence regulator *oxyR* (vGI-6, or MAP1631 to MAP1637) (30); and a region containing the F57 diagnostic gene (vGI-4, or MAP0851 to MAP0866) (34). Differences in ratios obtained from vGIs in *M. avium* subsp. *paratuberculosis* type I and type III isolates were significantly less than those observed with LSPs between *M. avium* subsp. *paratuberculosis* K-10 and *M. avium* subsp. *hominissuis* 104 and were often close to threshold values derived during normalization against the complete genome data set. However, the varied morphological appearances observed with *M. avium* subsp. *paratuberculosis* type III strains grown on solid media suggested that these cultures contained a mixture of variant forms, mostly of the rough type, exhibiting low and high rates of growth. We hypothesized that the total genomic DNA ex-

tracted for array analysis from a mixture of colonies with variations in duplications or deletions would contain a heterogeneous population of genomes that could generate the types of fluctuations in signals we have observed. Therefore, to confirm that these subtle, potentially mixed signal differences were significant and not a hybridization phenomenon perhaps associated with low GC%, we designed gene-specific qPCRs directed at ORFs inside vGI regions and showed that three of the four vGI regions tested had significant increases in *M. avium* subsp. *paratuberculosis* type III strains in comparison with *M. avium* subsp. *paratuberculosis* type II strains. It was of particular interest that one vGI region (MAP2443 to MAP2457) included the ribosomal (*rrn*) operon and that qPCR directed against a 16S pre-*rrn* region of the genome showed significant increases ($P = 0.037$) in overall copy number from *M. avium* subsp. *paratuberculosis* type III strains over that from *M. avium* subsp. *paratuberculosis* type II strains. Importantly, the differences in signals observed from vGI-associated genes were significantly less than the increases observed from a known gene duplication included as a control (MAP2729 in vaccine strain II). This suggested that the variation of signal in vGI regions occurs in only a proportion of the bacterial population within each culture and represents either a mixed population of fixed deletions and duplications or possibly a combination of transient variations induced during particular growth phases. We thus compared vGI qPCR signals from single large and small colonies picked from the same culture slant. The results obtained from this analysis indicated significant increases in vGI copy number in large colonies over that in small colonies in *M. avium* subsp. *paratuberculosis* type III strain CAM86 but not in two *M. avium* subsp. *paratuberculosis* type II strains, suggesting an association with growth phenotype and a potential for variability between *M. avium* subsp. *paratuberculosis* types.

Significantly, 11 of 16 vGIs were found to be immediately flanked by insertion sequences, including IS*900*, IS*1311*, and integrases associated with phage elements. In addition, both *M. avium* subsp. *paratuberculosis* type I and type III strains but none of the type II strains contained the insertion sequence IS*6120* (MAV_2223). This element is present in other mycobacteria, including *M. avium* subsp. *hominissuis* 104 (seven copies) and *Mycobacterium smegmatis* (two copies). The potential to control the variation in gene copy number in vGIs through mechanisms involving transpositional elements resulting in genomic duplications and deletions would significantly increase the adaptability of any strain. The presence of multiple vGIs in *M. avium* subsp. *paratuberculosis* type I and type III strains indicates that a range of factors could be influenced by these genomic rearrangements and that fluctuations in transposase activity, if acting in this way, may effect a crude form of global gene control.

In conclusion, this study defines the genomic diversity among the three major groups of *M. avium* subsp. *paratuberculosis*. It shows that *M. avium* subsp. *paratuberculosis* type I and type III strains contain a larger genomic complement than *M. avium* subsp. *paratuberculosis* type II strains and these additional regions encode ORFs with the putative functional capacity to promote different phenotypic characteristics that may result in alterations of disease pathogenesis. The increased potential for plasticity provided by vGIs suggests that previously undescribed mechanisms may exist in *M. avium* subsp. *paratuberculosis*, increasing adaptability through transient genomic alterations. Further work is necessary to clarify the significance of these comparisons and the influences they may have on mechanisms of strain/host adaptation.

REFERENCES

1. **Becq, J., M. C. Gutierrez, V. Rosas-Magallanes, J. Rauzier, B. Gicquel, O. Neyrolles, and P. Deschavanne.** 2007. Contribution of horizontally acquired genomic islands to the evolution of the tubercle bacilli. Mol. Biol. Evol. **24:**1861–1871.
2. **Behr, M. A., and V. Kapur.** 2008. The evidence for *Mycobacterium paratuberculosis* in Crohn's disease. Curr. Opin. Gastroenterol. **24:**17–21.
3. **Belisle, J. T., K. Klaczkiewicz, P. J. Brennan, W. R. Jacobs, Jr., and J. M. Inamine.** 1993. Rough morphological variants of *Mycobacterium avium*. Characterization of genomic deletions resulting in the loss of glycopeptidolipid expression. J. Biol. Chem. **268:**10517–10523.
4. **Bull, T. J., E. J. McMinn, K. Sidi-Boumedine, A. Skull, D. Durkin, P. Neild, G. Rhodes, R. Pickup, and J. Hermon-Taylor.** 2003. Detection and verification of *Mycobacterium avium* subsp. *paratuberculosis* in fresh ileocolonic mucosal biopsy specimens from individuals with and without Crohn's disease. J. Clin. Microbiol. **41:**2915–2923.
5. **Casali, N., and L. W. Riley.** 2007. A phylogenomic analysis of the *Actinomycetales* mce operons. BMC Genomics **8:**60.
6. **Castellanos, E., A. Aranaz, B. Romero, L. de Juan, J. Alvarez, J. Bezos, S. Rodríguez, K. Stevenson, A. Mateos, and L. Domínguez.** 2007. Polymorphisms in *gyrA* and *gyrB* genes among *Mycobacterium avium* subsp. *paratuberculosis* type I, II, and III isolates. J. Clin. Microbiol. **45:**3439–3442.
7. **Collins, D. M., D. M. Gabric, and G. W. de Lisle.** 1990. Identification of two groups of *Mycobacterium paratuberculosis* strains by restriction endonuclease analysis and DNA hybridization. J. Clin. Microbiol. **28:**1591–1596.
8. **de Juan, L., J. Alvarez, A. Aranaz, A. Rodriguez, B. Romero, J. Bezos, A. Mateos, and L. Dominguez.** 2006. Molecular epidemiology of types I/III strains of *Mycobacterium avium* subspecies *paratuberculosis* isolated from goats and cattle. Vet. Microbiol. **115:**102–110.
9. **de Juan, L., J. Alvarez, B. Romero, J. Bezos, E. Castellanos, A. Aranaz, A. Mateos, and L. Dominguez.** 2006. Comparison of four different culture media for isolation and growth of type II and type I/III *Mycobacterium avium* subsp. *paratuberculosis* strains isolated from cattle and goats. Appl. Environ. Microbiol. **72:**5927–5932.
10. **de Juan, L., A. Mateos, L. Dominguez, J. M. Sharp, and K. Stevenson.** 2005. Genetic diversity of *Mycobacterium avium* subspecies *paratuberculosis* isolates from goats detected by pulsed-field gel electrophoresis. Vet. Microbiol. **106:**249–257.
11. **Dohmann, K., B. Strommenger, K. Stevenson, L. de Juan, J. Stratmann, V. Kapur, T. J. Bull, and G. F. Gerlach.** 2003. Characterization of genetic differences between *Mycobacterium avium* subsp. *paratuberculosis* type I and type II isolates. J. Clin. Microbiol. **41:**5215–5223.
12. **Dorrell, N., J. A. Mangan, K. G. Laing, J. Hinds, D. Linton, H. Al-Ghusein, B. G. Barrell, J. Parkhill, N. G. Stoker, A. V. Karlyshev, P. D. Butcher, and B. W. Wren.** 2001. Whole genome comparison of *Campylobacter jejuni* human isolates using a low-cost microarray reveals extensive genetic diversity. Genome Res. **11:**1706–1715.
13. **Eisen, M. B., P. T. Spellman, P. O. Brown, and D. Botstein.** 1998. Cluster analysis and display of genome-wide expression patterns. Proc. Natl. Acad. Sci. USA **95:**14863–14868.
14. **Feller, M., K. Huwiler, R. Stephan, E. Altpeter, A. Shang, H. Furrer, G. E. Pfyffer, T. Jemmi, A. Baumgartner, and M. Egger.** 2007. *Mycobacterium avium* subspecies *paratuberculosis* and Crohn's disease: a systematic review and meta-analysis. Lancet Infect. Dis. **7:**607–613.
15. **Gioffre, A., E. Infante, D. Aguilar, M. P. Santangelo, L. Klepp, A. Amadio, V. Meikle, I. Etchechoury, M. I. Romano, A. Cataldi, R. P. Hernandez, and F. Bigi.** 2005. Mutation in mce operons attenuates *Mycobacterium tuberculosis* virulence. Microbes Infect. **7:**325–334.
16. **Griffiths, T. A., K. Rioux, and J. De Buck.** 2008. Sequence polymorphisms in a surface PPE protein distinguish types I, II, and III of *Mycobacterium avium* subsp. *paratuberculosis*. J. Clin. Microbiol. **46:**1207–1212.
17. **Harris, N. B., and R. G. Barletta.** 2001. *Mycobacterium avium* subsp. *paratuberculosis* in veterinary medicine. Clin. Microbiol. Rev. **14:**489–512.
18. **Hermon-Taylor, J., and T. Bull.** 2002. Crohn's disease caused by *Mycobacterium avium* subspecies *paratuberculosis*: a public health tragedy whose resolution is long overdue. J. Med. Microbiol. **51:**3–6.
19. **Hinds, J., K. G. Laing, J. A. Mangan, and P. D. Butcher.** 2002. Glass slide microarrays for bacterial genomes, p. 83–89. *In* B. W. Wren and N. Dorrell (ed.), Methods in microbiology: functional microbial genomics. Academic Press, London, United Kingdom.
20. **Hinds, J., A. A. Witney, and J. K. Vass.** 2002. Microarray design for bacterial genomes, p. 67–82. *In* B. W. Wren and N. Dorrell (ed.), Methods in microbiology: functional microbial genomics. Academic Press, London, United Kingdom.

21. **Horan, K. L., R. Freeman, K. Weigel, M. Semret, S. Pfaller, T. C. Covert, D. van Soolingen, S. C. Leão, M. A. Behr, and G. A. Cangelosi.** 2006. Isolation of the genome sequence strain *Mycobacterium avium* 104 from multiple patients over a 17-year period. J. Clin. Microbiol. **44:**783–789.
22. **Kennedy, D. J., and G. Benedictus.** 2001. Control of *Mycobacterium avium subsp. paratuberculosis* infection in agricultural species. Rev. Sci. Tech. **20:** 151–179.
23. **Li, L., J. P. Bannantine, Q. Zhang, A. Amonsin, B. J. May, D. Alt, N. Banerji, S. Kanjilal, and V. Kapur.** 2005. The complete genome sequence of *Mycobacterium avium* subspecies *paratuberculosis*. Proc. Natl. Acad. Sci. USA **102:**12344–12349.
24. **Marsh, I. B., J. P. Bannantine, M. L. Paustian, M. L. Tizard, V. Kapur, and R. J. Whittington.** 2006. Genomic comparison of *Mycobacterium avium* subsp. *paratuberculosis* sheep and cattle strains by microarray hybridization. J. Bacteriol. **188:**2290–2293.
25. **Maslow, J. N., D. Dawson, E. A. Carlin, and S. M. Holland.** 1999. Hemolysin as a virulence factor for systemic infection with isolates of *Mycobacterium avium* complex. J. Clin. Microbiol. **37:**445–446.
26. **Motiwala, A. S., H. K. Janagama, M. L. Paustian, X. Zhu, J. P. Bannantine, V. Kapur, and S. Sreevatsan.** 2006. Comparative transcriptional analysis of human macrophages exposed to animal and human isolates of *Mycobacterium avium* subspecies *paratuberculosis* with diverse genotypes. Infect. Immun. **74:**6046–6056.
27. **Mustafa, T., H. G. Wiker, O. Morkve, and L. Sviland.** 2008. Differential expression of mycobacterial antigen MPT64, apoptosis and inflammatory markers in multinucleated giant cells and epithelioid cells in granulomas caused by *Mycobacterium tuberculosis*. Virchows Arch. **452:**449–456.
28. **Naser, S. A., G. Ghobrial, C. Romero, and J. F. Valentine.** 2004. Culture of *Mycobacterium avium* subspecies *paratuberculosis* from the blood of patients with Crohn's disease. Lancet **364:**1039–1044.
29. **Newton, R., J. Hinds, and L. Wernisch.** 2006. A hidden Markov model web application for analysing bacterial genomotyping DNA microarray experiments. Appl. Bioinformatics **5:**211–218.
30. **Pagán-Ramos, E., S. S. Master, C. L. Pritchett, R. Reimschuessel, M. Trucksis, G. S. Timmins, and V. Deretic.** 2006. Molecular and physiological effects of mycobacterial *oxyR* inactivation. J. Bacteriol. **188:**2674–2680.
31. **Paustian, M. L., V. Kapur, and J. P. Bannantine.** 2005. Comparative genomic hybridizations reveal genetic regions within the *Mycobacterium avium* complex that are divergent from *Mycobacterium avium* subsp. *paratuberculosis* isolates. J. Bacteriol. **187:**2406–2415.
32. **Paustian, M. L., X. Zhu, S. Sreevatsan, S. Robbe-Austerman, V. Kapur, and J. P. Bannantine.** 2008. Comparative genomic analysis of *Mycobacterium avium* subspecies obtained from multiple host species. BMC Genomics **9:**135.
33. **Pavlik, I., A. Horvathova, L. Dvorska, J. Bartl, P. Svastova, R. du Maine, and I. Rychlik.** 1999. Standardisation of restriction fragment length polymorphism analysis for *Mycobacterium avium* subspecies *paratuberculosis*. J. Microbiol. Methods **38:**155–167.
34. **Poupart, P., M. Coene, H. Van Heuverswyn, and C. Cocito.** 1993. Preparation of a specific RNA probe for detection of *Mycobacterium paratuberculosis* and diagnosis of Johne's disease. J. Clin. Microbiol. **31:**1601–1605.
35. **Semret, M., D. C. Alexander, C. Y. Turenne, P. de Haas, P. Overduin, D. van Soolingen, D. Cousins, and M. A. Behr.** 2005. Genomic polymorphisms for *Mycobacterium avium* subsp. *paratuberculosis* diagnostics. J. Clin. Microbiol. **43:**3704–3712.
36. **Semret, M., C. Y. Turenne, P. de Haas, D. M. Collins, and M. A. Behr.** 2006. Differentiating host-associated variants of *Mycobacterium avium* by PCR for detection of large sequence polymorphisms. J. Clin. Microbiol. **44:**881–887.
37. **Semret, M., G. Zhai, S. Mostowy, C. Cleto, D. Alexander, G. Cangelosi, D. Cousins, D. M. Collins, D. van Soolingen, and M. A. Behr.** 2004. Extensive genomic polymorphism within *Mycobacterium avium*. J. Bacteriol. **186:**6332–6334.
38. **Senaratne, R. H., B. Sidders, P. Sequeira, G. Saunders, K. Dunphy, O. Marjanovic, J. R. Reader, P. Lima, S. Chan, S. Kendall, J. McFadden, and L. W. Riley.** 2008. *Mycobacterium tuberculosis* strains disrupted in mce3 and mce4 operons are attenuated in mice. J. Med. Microbiol. **57:**164–170.
39. **Stevenson, K., V. M. Hughes, L. de Juan, N. F. Inglis, F. Wright, and J. M. Sharp.** 2002. Molecular characterization of pigmented and nonpigmented isolates of *Mycobacterium avium* subsp. *paratuberculosis*. J. Clin. Microbiol. **40:**1798–1804.
40. **Stratmann, J., B. Strommenger, R. Goethe, K. Dohmann, G. F. Gerlach, K. Stevenson, L. L. Li, Q. Zhang, V. Kapur, and T. J. Bull.** 2004. A 38-kilobase pathogenicity island specific for *Mycobacterium avium* subsp. *paratuberculosis* encodes cell surface proteins expressed in the host. Infect. Immun. **72:**1265–1274.
41. **Witney, A. A., G. L. Marsden, M. T. Holden, R. A. Stabler, S. E. Husain, J. K. Vass, P. D. Butcher, J. Hinds, and J. A. Lindsay.** 2005. Design, validation, and application of a seven-strain *Staphylococcus aureus* PCR product microarray for comparative genomics. Appl. Environ. Microbiol. **71:**7504–7514.
42. **Wu, C. W., J. Glasner, M. Collins, S. Naser, and A. M. Talaat.** 2006. Whole-genome plasticity among *Mycobacterium avium* subspecies: insights from comparative genomic hybridizations. J. Bacteriol. **188:**711–723.